

Targeted Disruption of *Tgif*, the Mouse Ortholog of a Human Holoprosencephaly Gene, Does Not Result in Holoprosencephaly in Mice†

Jun Shen and Christopher A. Walsh*

Howard Hughes Medical Institute, Department of Neurology, Beth Israel Deaconess Medical Center, and Program in Neuroscience, Division of Medical Sciences, Graduate School of Arts and Sciences, Harvard University, Boston, Massachusetts 02115

Received 8 January 2005/Accepted 5 February 2005

5'-TG-3'-interacting factor or transforming growth factor beta (TGF- β)-induced factor (TGIF) belongs to a family of evolutionarily conserved proteins that are characterized by an atypical three-amino-acid loop extension homeodomain. In vitro studies have implicated TGIF as a transcriptional repressor and corepressor in retinoid and TGF- β signaling pathways that regulate several important biological processes. Heterozygous nonsense and missense mutations of the human *TGIF* gene have been associated with holoprosencephaly, the most common congenital malformation of the forebrain. In mice, *Tgif* mRNA is expressed ubiquitously in the ventricular neuroepithelium at embryonic day 10.5 (E10.5) but displays a medial to lateral gradient in the developing cerebral cortex at E12.5. The expression quickly declines by E14.5. The spatiotemporal expression profile of *Tgif* is consistent with its involvement in midline forebrain development. To better understand the function of *Tgif* in forebrain patterning and proliferation in vivo, we generated mice lacking *Tgif* by targeted deletion of exons 2 and 3, which encode 98% of the amino acids. *Tgif*^{-/-} mice had no detectable Tgif protein by Western blotting. Surprisingly, however, these mice were viable and fertile. In addition, there were no discernible derangements in any of the major organ systems, including the forebrain. Overall our results point to a possible functional redundancy of Tgif, potentially provided by the closely related Tgif2.

5'-TG-3'-interacting factor or transforming growth factor beta (TGF- β)-induced factor (TGIF) is a member of the evolutionarily conserved three-amino-acid loop extension (TALE) superclass of atypical homeodomain proteins (4). The *Drosophila* genome contains two tandemly repeated *TGIF*-like genes, *achintya* and *vismay* (2). Loss of both *achintya* and *vismay* results in male infertility due to defects in spermatogenesis (2, 48). These two genes have redundant functions, because either *achintya* or *vismay* can rescue the phenotype (48). While the homology of human TGIF and *Drosophila* TGIF-like proteins is restricted to the TALE homeodomain, the entire genomic region of *TGIF* is highly conserved in mammals. The genomic exon and intron organization of *TGIF* is identical in humans and mice. Furthermore, human and mouse TGIF are 82% and 90% identical at the mRNA and protein levels, respectively. Since mammalian *TGIF* and *Drosophila* *TGIF*-like genes are very different outside of the homeodomain, it suggests that mammalian TGIF may have unique functions.

Although *Drosophila* *achintya* and *vismay* are transcriptional activators (20), mammalian TGIF has been implicated as a transcriptional repressor and corepressor based on in vitro studies (32, 50). TGIF exhibits several different modes of re-

pression (51). First, TGIF represses transcription by competing with retinoid receptors for the DNA binding sites, the retinoid X receptor (RXR) responsive element, in the promoter regions of the regulated genes (4, 18, 23). Second, TGIF represses transcription by acting as a Smad corepressor (50). Smad proteins are the cellular signaling transducers of the TGF- β signaling pathway (22). Upon TGF- β family ligand binding to the cell surface receptor serine/threonine kinases, the receptor multimerizes and phosphorylates Smad proteins (28). The phosphorylation-activated Smad proteins then translocate to the nucleus to activate gene expression by interacting with coactivators (29, 45). TGIF replaces the coactivators to bind to Smad2 and Smad3 and also recruits other general corepressors, including histone deacetylases (HDACs) and Sin3, to the complex, thus repressing TGF- β -activated transcription (44, 49). In addition, TGIF may also regulate ubiquitin-dependent degradation of Smad2 (43). Third, TGIF can repress gene expression by recruiting CtBP, which may repress transcription via interactions with polycomb group proteins (32).

Mutations in the human *TGIF* gene have been associated with holoprosencephaly (HPE [MIM 236100]). HPE is the most common congenital malformation of the developing human forebrain, in which the two cerebral hemispheres fail to separate and the two lateral ventricles are fused into one (13, 30, 39, 41). Heterozygous nonsense and missense mutations in the genes *SIX3*, *SHH*, *TGIF*, *ZIC2*, and *PTCH* have been identified to be responsible for familial HPE2, HPE3, HPE4, HPE5, and HPE7, respectively (3, 7, 16, 33, 47). *TGIF* falls within the minimal critical region of the HPE4 locus (HPE4 [MIM 142946]) on human chromosome 18p11.3 (40). Six mis-

* Corresponding author. Mailing address: Howard Hughes Medical Institute, Department of Neurology, Beth Israel Deaconess Medical Center, NRB 266, 77 Avenue Louis Pasteur, Boston, MA 02115. Phone: (617) 667-0813. Fax: (617) 667-0815. E-mail: cwalsh@bidmc.harvard.edu.

† Supplemental material for this article may be found at <http://mcb.asm.org/>.

sense mutations and one nonsense heterozygous mutation in *TGIF* have been reported in HPE patients to date (1, 8, 16, 25). The nonsense mutation generates an early stop codon within the homeodomain (1). HPE has been identified in partial chromosome 18p deletion cases, which implicates that HPE4 may result from partial loss of *TGIF* function (10, 17, 36). On the other hand, HPE4 has also been implied in partial trisomy 18 cases, which suggests a gain-of-function mechanism (9, 26, 52). It remains unclear how *TGIF* mutations cause HPE. Whereas targeted disruption of *Shh*, *Zic2*, or *Six3* in mice results in HPE-like malformation of the forebrain (12, 24, 37), we report here that *Tgif*^{-/-} mice are, surprisingly, viable, fertile, and indistinguishable from wild-type littermates.

MATERIALS AND METHODS

Animals. All protocols involving the use of animals were in compliance with the National Institutes of Health's *Guide for the Care and Use of Laboratory Animals* and the Harvard University Institutional Animal Care and Use Committee. C57BL/6J (B6), FVB/N-TgN(Actb-cre)2Mrt (Actb-Cre), and STOCK *Shh^{tm1Amc/J}* (*Shh*^{+/-}) mouse strains were imported from Jackson Laboratory (Bar Harbor, ME). For time-pregnant mice and embryos, the noon of the day that the vaginal plug was observed was designated gestation day 0.5 (GD 0.5) or embryonic day 0.5 (E0.5).

ISH. For in situ hybridization (ISH), time-pregnant mice were sacrificed by carbon dioxide euthanasia. The embryos were dissected in cold 0.01 M phosphate-buffered saline (PBS) (pH 7.4). For section ISH, the heads of the embryos were immediately frozen in isopentane on dry ice and stored at -80°C until processed. The embryonic heads were sectioned coronally at 16 µm in a cryostat, mounted on Superfrost plus microscope slides (Fisher Scientific, Pittsburgh, PA), and stored at -80°C until processed. For whole-mount ISH, whole embryos were fixed in 4% paraformaldehyde, dehydrated with methanol, and stored at -20°C in 100% methanol for up to 3 months.

Nonradioactive ISH was performed using digoxigenin-labeled cRNA probes as previously described (15, 35). The *Shh* probes were derived from a cDNA clone (courtesy of C. Tabin) as described previously (14). For the *Tgif* probes, a SalI-digested expressed sequence tag clone (IMAGE:3595273; Invitrogen, Carlsbad, CA) of *Tgif* was used as the linearized template. *Tgif* antisense cRNA probes were in vitro transcribed with T7 RNA polymerase. For the *Tgif2* probes, a 333-bp fragment of *Tgif2* cDNA (nucleotide positions 381 to 724 downstream of the ATG start site) was amplified by PCR (forward primer, 5'-CTCCTGTCTGTGTGCTCCA-3'; reverse primer, 5'-GCGTTTTCTGAGACGAAAGG-3') and cloned in the pCRII vector (Invitrogen, Carlsbad, CA). The primers were designed using Primer3 (42). The *Tgif2* partial cDNA clone was linearized with EcoRV and transcribed with Sp6 RNA polymerase to generate the *Tgif2* antisense probes. All probe templates were verified by direct sequencing. Sections or whole embryos were hybridized to each probe (~100 ng/ml) at 68°C overnight. Hybridized probes were visualized using alkaline phosphatase-conjugated anti-digoxigenin Fab fragments and BM Purple (Roche, Indianapolis, IN) or 5-bromo-4-chloro-3-indolyl-phosphate/Nitro Blue Tetrazolium substrate (Kierkegaard and Perry Laboratories, Gaithersburg, MD).

Construction of the *Tgif* targeting vector, embryonic stem (ES) cell screening using Southern blotting, and generation of *Tgif* mutant mice. The genomic clones corresponding to the mouse *Tgif* locus were isolated from a genomic library prepared from the 129/SvEV mouse strain (courtesy of M. Thompson) by using a mouse *Tgif* probe of the 899-bp intron between the last two coding exons. The 11-kb *Tgif* genomic fragment from ClaI to BclI including all exons was subcloned into a modified pSP72 vector. For the targeting vector, a 2.2-kb region of genomic DNA containing exons 2 and 3 of the *Tgif* gene was flanked by two *loxP* sites. A selectable cassette containing the genes for neomycin resistance (Neo cassette) was inserted downstream of the genomic fragment flanked by two FRT sites (InGenious Targeting, Stony Brook, NY). The *Tgif* targeting construct was electroporated into ES cells that were subsequently grown in medium containing G418 to select for cells with homologous recombination. Correctly targeted ES cell clones were identified by Southern analysis. Genomic DNA was digested with PstI and identified by a 3' probe downstream of the targeted *Tgif* locus or digested with PacI and KpnI and identified by a 5' probe upstream of the targeted *Tgif* locus. Two independent ES cell clones with the targeted *Tgif* locus were injected into B6 blastocysts to generate two lines of chimeras (MGH Gene

Targeting Core, Charlestown, MA). The chimeras were crossed into B6 mice for germ line transmission (*Tgif^{loxPneo}*). The Neo cassette was deleted by crossing the mice into human β-actin-driven FLPe deleter mice (courtesy of S. Dymecki) to generate the *Tgif^{loxP}* conditional line. The null allele (*Tgif*⁻) was generated by crossing the *Tgif^{loxP}* line into the human β-actin-driven Cre deleter line. Germ line transmission of the targeted allele (*Tgif^{loxPneo}*), the conditional allele (*Tgif^{loxP}*), and the null allele (*Tgif*⁻) in mice was confirmed by Southern blotting. Genomic DNA was digested with SpeI and identified by a 3' probe downstream of the targeted *Tgif* locus. The accession number for this mouse line is MGI: 3513135.

Genotyping of *Tgif* wild-type, conditional, and null alleles by genomic PCR. Mouse biopsy samples were collected and digested with 10 µg proteinase K in 100 µl buffer (50 mM KCl, 10 mM Tris-HCl, pH 8.3, 2.5 mM MgCl₂, 0.1 mg/ml gelatin, 0.45% [vol/vol] Nonidet P-40, and 0.45% [vol/vol] Tween 20) at 55°C overnight. Genomic DNA (0.5 µl) containing solution was used in 10 µl PCR mixture including 0.5 U of *Taq* (QIAGEN, Valencia, CA), 1× PCR buffer, 0.125 mM deoxynucleotide triphosphates (Invitrogen, Carlsbad, CA), 1.5 mM MgCl₂, and primers (1 µM 1f, 5'-TAACAGCAAGCCTTTCACGA-3'; 0.35 µM 1r, 5'-GCCCTCACACCTTGCTTTT-3'; and 0.65 µM 2r, 5'-TGGCCCTTCT-GAAATACAC-3'; Sigma-Genosys, The Woodlands, TX). The PCR cycle profile was as follows: 1 cycle at 94°C for 5 min, followed by 35 cycles at 94°C for 30 s, 60°C for 45 s, and 72°C for 1 min, and finally 1 cycle at 72°C for 10 min. Primers 1f and 1r surrounding the first *loxP* insertion site would amplify a 112-bp fragment of the wild-type allele and a 174-bp fragment of the conditional allele. Primers 1f and 2r (downstream of the Neo cassette insertion site) would amplify a 313-bp fragment of null allele.

Western analysis. Total protein was extracted from embryonic mouse tissue. Mouse embryos were immediately frozen in liquid nitrogen. Tissues were homogenized in protein extraction buffer containing 100 mM Tris, pH 6.8, 2% sodium dodecyl sulfate (SDS), 25 mM dithiothreitol, and protease inhibitors. Proteins were separated on SDS-20% polyacrylamide electrophoresis gels and transferred to Immobilon-P polyvinylidene difluoride membranes (Millipore, Billerica, MA). Western blots were blocked in 3% dry milk for 2 h at room temperature, incubated with a rabbit polyclonal antiserum against TGIF (TGIF H-172; Santa Cruz Biotechnology, Santa Cruz, CA) or against tubulin as a control at 4°C overnight, followed by incubation with horseradish peroxidase-conjugated secondary antibodies at room temperature, and detected by the ECL detection kit (Amersham, Piscataway, NJ).

Histological analysis. Four-week-old wild-type, heterozygous, and *Tgif*^{-/-} mice were weighed and sacrificed by carbon dioxide euthanasia. Sixty mice (10 per sex per genotype) were examined. The body length and tail length were measured with a ruler. The major organs were dissected, examined, rinsed with PBS, blotted dry, and weighed on a digital scale. For histology, 4- and 7-week-old age- and sex-matched wild-type, heterozygous, and *Tgif*^{-/-} mice were anesthetized with 20 µl avertin per gram body weight via intraperitoneal injection. Avertin was prepared by dissolving 1.25 mg 2,2,2-tribromoethanol (Sigma-Aldrich, St. Louis, MO) in 2.5 ml 2.5% 2-methyl-2-butanol (Fisher Scientific, Pittsburgh, PA) water solution. The anesthetized mice were perfused transcardially with PBS, followed by Bouin's solution (Sigma-Aldrich, St. Louis, MO). Tissues from various organs were dissected and fixed in Bouin's fixative. Tissue samples were processed routinely and embedded in paraffin, sectioned at 5 µm, stained with hematoxylin and eosin (Harvard Medical School Rodent Histopathology Core and BIDMC Histology Core, Boston, MA), and analyzed by light microscopy.

Retinoic acid treatment. *Tgif*^{-/-} female mice were mated with *Tgif*^{+/-} male mice overnight. The time-pregnant mice were weighed and fed with 7.5 mg/kg body weight all-*trans*-retinoic acid (ATRA) (Sigma-Aldrich, St. Louis, MO) suspended in 100 µl canola oil at 9 a.m. on GD 7. The ATRA-treated pregnant mice were sacrificed by carbon dioxide euthanasia in the late afternoon of GD11. The embryos were dissected and genotyped by PCR. The morphology of each embryo was examined and recorded.

RESULTS

Expression patterns of *Tgif* in mouse embryos during early development. Mouse *Tgif* mRNA is detected in the whole embryo from E7 by reverse transcription-PCR and Northern blotting and in the external granular layer of the cerebellum as well as the neuroepithelium of the hippocampus at E16 by ISH (5). The expression of mouse *Tgif* mRNA has also been reported in

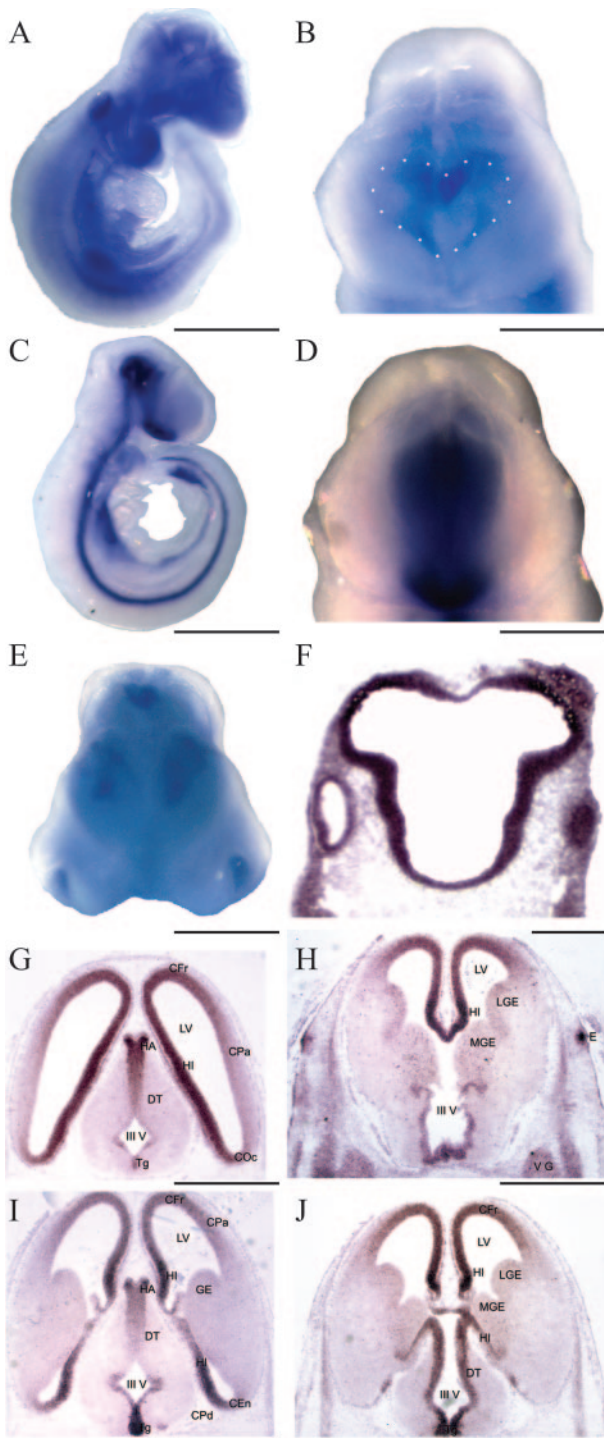


FIG. 1. The expression patterns of *Tgif* mRNA in E9.5 to E12.5 wild-type mouse embryos by ISH. The expression pattern of *Tgif* in the E9.5 wild-type mouse whole embryo (A) is different than that of *Shh*, another HPE gene (C). Enlarged front views of the same embryos are shown in panel B (of panel A) and panel D (of panel C). *Tgif* is ubiquitously expressed in the forebrain, with the highest expression in the heart-shaped ventricular lining indicated by the dotted line. At E10.5, *Tgif* is highly expressed in the forebrain and in the nasal pits as shown in panel E. E10.5 coronal sections show that *Tgif* is expressed in the ventricular neuroepithelium of the developing cerebral hemispheres (F). By E12.5, *Tgif* expression displayed a medial to lateral gradient at all rostral to caudal levels of the forebrain (G to J). CFr, frontal cortex; CEn, entorhinal cortex; COc, occipital cortex; CPa,

the E15 forebrain and in E9.5 to E10.5 embryos (16, 53). However, the exact spatiotemporal expression patterns of *Tgif* in the forebrain of early mouse embryos have not been described.

We performed whole-mount ISH on E9.5 and E10.5 mouse embryos. *Tgif* mRNA was widely expressed in the developing mouse embryo at E9.5 (Fig. 1A), with the highest expression in the forebrain, the branchial arches, the otic pit, and the limb buds, but not in the heart. The front view at a higher magnification revealed the highest expression in the heart-shaped ventricular lining of the bulging telencephalic hemispheres (Fig. 1B). The expression pattern of *Tgif* was very different from that of *Shh*, the human HPE3 gene (Fig. 1C and 1D). In E10.5 embryos, *Tgif* expression was high in the forebrain and in the nasal pits (Fig. 1E).

Since *Tgif* showed an interesting expression pattern inside of the forebrain, we performed ISH on coronal sections of E10.5 and E12.5 mouse embryos. *Tgif* expression was observed ubiquitously in the ventricular neuroepithelium but not in the head mesenchyme at E10.5 (Fig. 1F). At E12.5, *Tgif* expression was found in the ventricular neuroepithelium in a medial to lateral gradient at all rostral to caudal levels of the telencephalon examined (Fig. 1G to 1J). The expression is highest in the midline which would form the future hippocampus. The expression in the neocortical region gradually decreased from the more medial frontal cortex to the more lateral parietal cortex, and the expression in the lateral ganglionic eminence and medial ganglionic eminence was lower than in the cortex. By E14.5, the expression became low throughout the whole embryo (data not shown). The dynamic and distinctive expression pattern of *Tgif* during the critical period of cerebral hemisphere formation was consistent with its potential role in forebrain proliferation and midline patterning.

Generation of *Tgif*^{-/-} mice. The interesting expression patterns of *Tgif* prompted us to investigate the *in vivo* function of *Tgif*. We decided to create a mouse model lacking *Tgif*. Because most human HPE fetuses are spontaneously aborted and known mouse models lacking other HPE genes are embryonically lethal, we hypothesized that mice with a simple deletion of *Tgif* would probably die prenatally. Therefore, we employed a conditional knockout strategy using the *Cre/loxP* system to overcome the potential lethality.

We targeted the mouse *Tgif* locus in ES cells by homologous recombination. A detailed scheme for the targeting construct is shown in Fig. 2. Using this strategy, we obtained four correctly targeted ES clones from 191 G418-resistant clones (Fig. 3A). Two independent ES cell clones were injected, and germ line transmission of both *Tgif*^{loxPneo/+} lines was achieved. The *Tgif*^{loxP/+} conditional lines and the *Tgif*^{-/-} knockout lines were produced by subsequent breeding, as genotyped by PCR (Fig. 3C) and Southern blotting (Fig. 3B). *Tgif* protein, which migrates as a doublet around 30 kDa on SDS-polyacrylamide

parietal cortex; CPd, cerebral peduncle; DT, dorsal thalamus; E, eye; GE, ganglionic eminence; HA, habenula; HI, hippocampus; III V, third ventricle; LGE, lateral GE; LV, lateral ventricle; MGE, medial GE; Tg, tegmentum; V G, fifth (trigeminal) ganglion. Scale bars: 1 mm in A, C, and E; 500 μ m in panels B, D, and F; 2 mm in panels G to J.

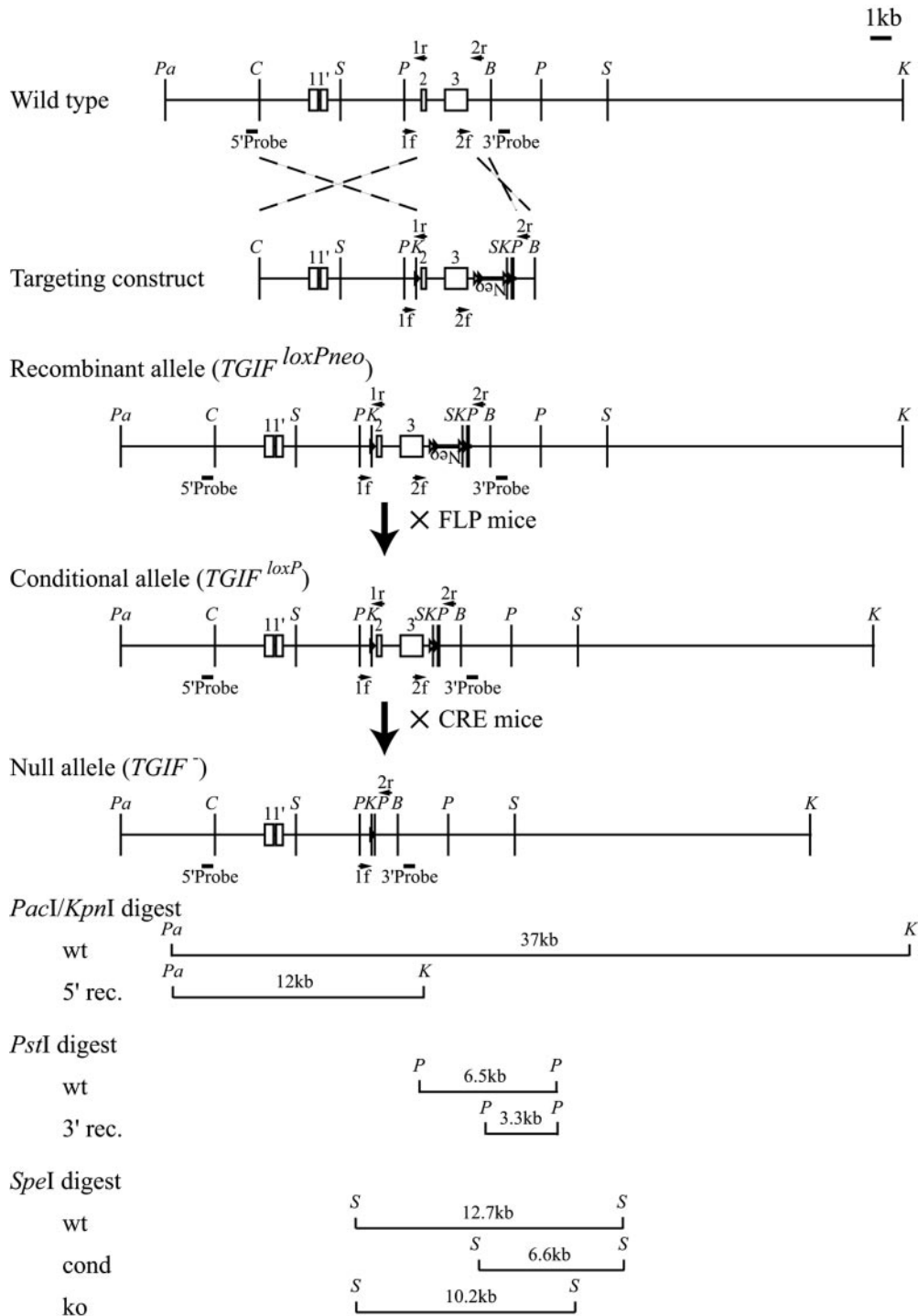


FIG. 2. Conditional knockout strategy for the targeted disruption of *Tgif* in mouse. The 11-kb *ClaI*-*BcgI* fragment containing all exons and introns of the mouse *Tgif* gene was subcloned. Exons are symbolized as numbered rectangles. Exon 1 encodes the first six amino acids. Alternative exon 1' contains the 5' untranslated region only, and this isoform uses the alternative start codon in exon 2. A targeting vector was constructed by inserting a *loxP* site 75 bp upstream of exon 2 and an inverted PGK-NEO cassette flanked with two FRT-*loxP* sites 181 bp downstream of exon 3 after the poly(A) signal. Filled and unfilled arrowheads represent the *loxP* and FRT sites, respectively. The conditional allele was generated in vivo by crossing with FLP deleter mice to remove the PGK-NEO cassette and one *loxP* site, which leaves two *loxP* sites flanking exon 2 and 3. The null allele was generated in vivo by subsequent crossing with CRE deleter mice to remove exons 2 and 3, which encode 98% of the amino acids in one isoform and 100% of the other. Short arrows labeled with 1f, 1r, 2f, and 2r indicate the positions of PCR primers. Short bars indicate the positions of the 5' and 3' probes used in Southern hybridizations. Vertical lines indicate the restriction sites: Pa, *PacI*; C, *ClaI*; S, *SpeI*; P, *PstI*; B, *BcgI*; and K, *KpnI*. Alleles: wt, wild type; 5' rec., 5' recombinant; 3' rec., 3' recombinant; cond, conditional; and ko, knockout.

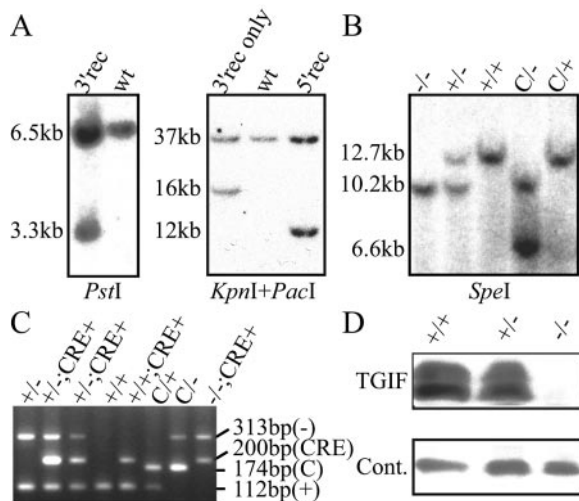


FIG. 3. Generation of *Tgif*^{-/-} mice. A. G418-resistant ES cells were screened for homologous recombination by Southern hybridization. A 3.3-kb PstI digest fragment was detected in 3' recombinant cells by the 3' probe (left panel). A 12-kb PacI-KpnI digest fragment was detected in 5' recombinant cells by 5' probe. The 16-kb fragment was produced by 3' recombination but not 5' recombination (right panel). B. Mice were genotyped by Southern hybridization. The *SpeI* fragments in the knockout, conditional, and wild-type alleles were 10.2 kb, 6.6 kb, and 12.7 kb, respectively. C. Mice were genotyped by PCR. The amplicon with primer pair 1f and 1r is 112 bp in the wild-type allele and 174 bp in the conditional allele. The amplicon with primer pair 1f and 2r is 313 bp in the null allele. D. *Tgif* protein was not detected in null embryos. Abbreviations: 3' rec, 3' recombinant ES cell; wt, wild type; 5' rec, 5' recombinant ES cell; +, wild-type allele; C, conditional allele; -, null allele; and Cont., control.

gels (27), was not detectable in *Tgif*^{-/-} embryos by Western blotting (Fig. 3D).

***Tgif*^{-/-} mice are viable and fertile.** Surprisingly, however, the mice lacking *Tgif* appeared normal. Breeding of *Tgif*^{+/-} mice resulted in approximately Mendelian ratios of progeny with no gender bias (Table 1). *Tgif*^{-/-} mice were indistinguishable from their wild-type and heterozygous littermates by gross observations. These mice displayed normal growth and home cage behaviors, including gait, general activity, grooming, and startle reflexes (Fig. 4). Both male and female *Tgif*^{-/-} mice were fertile. We set aside 8 wild-type, 8 heterozygous, and 10 knockout mice for long-term comparisons. One heterozygous mouse died at 5 months old with no obvious cause. The re-

maining 25 mice, including all 10 knockout mice, were still alive and indistinguishable from wild-type controls at 7 months of age when last examined.

Two *Tgif*^{-/-} mice, one male and one female, were sacrificed at the weaning age during our studies, because they displayed malocclusion of the teeth, which could be sporadic in C57BL/6J mice. One *Tgif*^{-/-} mouse had a kinked tail, but so did a wild-type littermate. One heterozygous mouse developed a solid tumor with a diameter of 1 cm near the right groin region at 4 months old, but the tumor receded by 6 months without any treatment. The mouse was still alive at 7 months of age when last examined. Therefore, these low-frequency events seemed unlikely to be attributable to *Tgif* deficiency.

Since *Tgif* was expected to play a role in forebrain patterning and proliferation, we performed morphological analysis of the brains of *Tgif*^{-/-} mice. The brains were normal in size and weight (Fig. 4B; also see Fig. S1A and S2A in the supplemental material). Major brain structures appeared normal (see Fig. S1A in the supplemental material). The midline structures, including the thalamus, the hypothalamus, and the pituitary gland, were maintained. The two cerebral hemispheres were well formed, and the two lateral ventricles were well separated (Fig. 4B; also see Fig. S1B in the supplemental material). Cerebral cortical lamination was preserved (Fig. 4C; also see Fig. S1D in the supplemental material). In addition, the lamination of the retina also appeared normal (Fig. 4D; also see Fig. S1E in the supplemental material). Histological analysis of other major organ systems, including the heart, the lungs, the mandibular glands, the thyroid glands, the esophagus, the stomach, the small intestines, the colon, the liver, the pancreases, the kidneys, the adrenal glands, the thymus, the spleen, the bones and bone marrow, the bladder, the ovaries, the uterus, and the testes, showed no discernible pathological dearrangements (see Fig. S2 in the supplemental material).

No direct genetic interaction between *Shh* and *Tgif*. Mutations in both *SHH* and *TGIF* have been found in a human HPE patient, whose mother, carrying only the *SHH* mutation, appeared phenotypically normal (16). This suggested that *SHH* and *TGIF* might interact genetically. We mated *Tgif*^{+/-} mice with *Shh*^{+/-} mice. Such a cross resulted in approximately Mendelian ratios of progeny (Table 1). *Tgif*^{-/-}; *Shh*^{+/-} mice were viable and fertile (Fig. 4A). The progeny of the intercross of *Tgif*^{-/-}; *Shh*^{+/-} mice also fit Mendelian ratios (Table 1). Furthermore, whole-mount ISH showed that *Tgif* mRNA was expressed in E10.5 *Shh*^{-/-} embryos, with the highest expression

TABLE 1. Progeny of *Tgif* mutant mice fit Mendelian ratio

Genotype		Gender of offspring	No. of offspring			Expected ratio
Sire	Dam		wt	<i>Tgif</i> ^{+/-}	<i>Tgif</i> ^{-/-}	
<i>Tgif</i> ^{+/-}	<i>Tgif</i> ^{+/-}	Male	24	48	28	100
		Female	26	50	26	102
		Total	50	98	54	202
<i>Shh</i> ^{+/-} ; <i>Tgif</i> ^{+/-}	<i>Shh</i> ^{+/-} ; <i>Tgif</i> ^{+/-}	Male	26	54	0	80
		Female	7	13	0	20
		Total	33	67	0	100

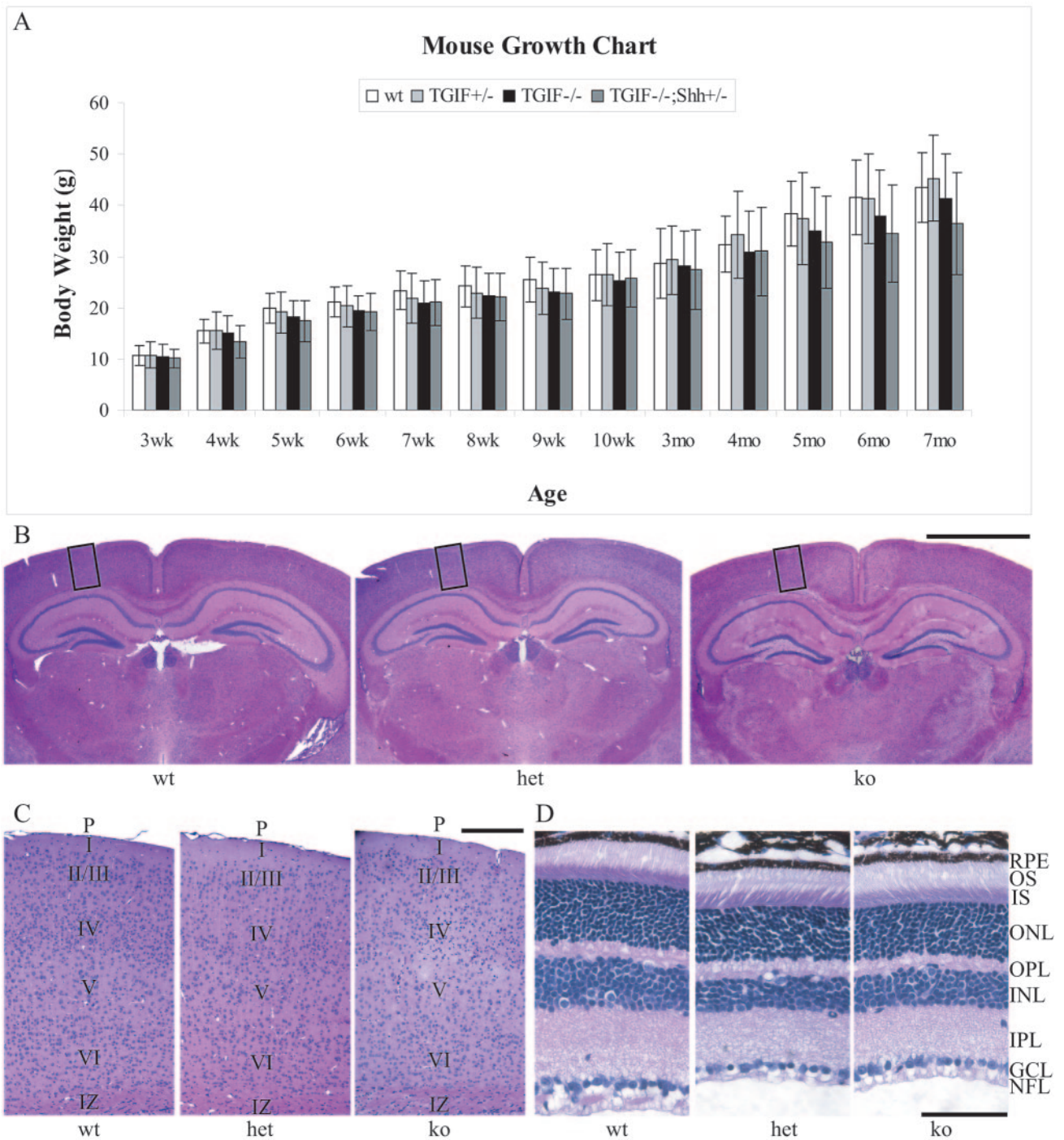


FIG. 4. Characterization of *Tgif*^{-/-} mice. A. The body weights of wild-type, heterozygous, and *Tgif*^{-/-} mice at various ages are graphed as Mean \pm 1 standard deviation. There is no significant difference among different genotype groups. B. The forebrains of 7-week-old *Tgif*^{-/-} mice are well separated into two hemispheres and indistinguishable from those of wild-type and heterozygous littermates. The boxed regions are enlarged in C. Scale bar, 1 mm. C. The lamination of the cerebral cortex is preserved in *Tgif*^{-/-} mice. I to VI, cortical layers I through VI; IZ, intermediate zone; P, pial surface. Scale bar, 125 μ m. D. The lamination of the retina is preserved in the eyes of 7-week-old *Tgif*^{-/-} mice. GCL, ganglion cell layer; INL, inner nuclear layer; IPL, inner plexiform layer; IS, inner segments; NFL, nerve fiber layer; ONL, outer nuclear layer; OPL, outer plexiform layer; OS, outer segments; RPE, retinal pigment epithelium. Scale bar, 62.5 μ m.

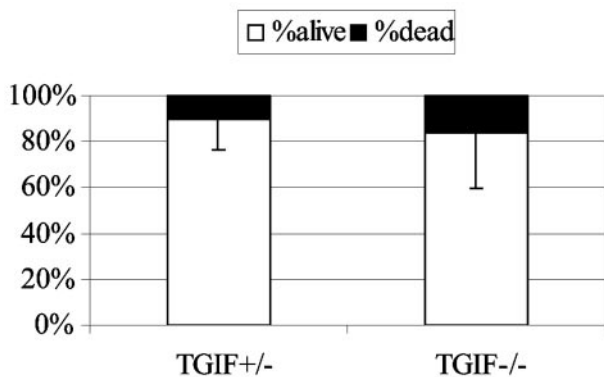


FIG. 5. The teratogenic effect of retinoic acid is not altered in *Tgif*^{-/-} embryos. Time-pregnant mice were treated with all-*trans* retinoic acid at GD 7. The embryos were analyzed at E11.75. The percentages of dead and live embryos in each genotype group are graphed. $n = 10$ litters; $P = 0.46$ by two-tailed Student *t* test.

in the primitive forebrain, the branchial arches, the otic pit, and the limb buds comparable to that of wild-type embryos (see Fig. S3 in the supplemental material). Tgif protein was detected in E11.5 and E12.5 *Shh*^{-/-} embryos (see Fig. S3 in the supplemental material). We also observed *Tgif*^{-/-}; *Shh*^{-/-} double-mutant embryos from E10.5 to E13.5. These double-deficient embryos were indistinguishable from *Shh*^{-/-} embryos. These results did not provide evidence to support the hypothesis that *Shh* and *Tgif* had direct genetic interaction in mouse.

Unaltered susceptibility to retinoic acid induced teratogenic effects. Mice that ingest ATRA during early pregnancy are more likely to produce HPE offspring (46). ATRA could activate RXR. Since TGIF represses RXR function, *TGIF* mutations in humans may cause HPE by deregulating the retinoid signaling pathway. If this were the case, ATRA would have a more potent teratogenic effect on *Tgif*^{-/-} embryos than on *Tgif*^{+/-} embryos. To test this hypothesis, we fed ATRA to time-pregnant *Tgif*^{-/-} mice on GD 7 and examined the phenotypes of the embryos in the late afternoon of GD 11. We collected 10 litters of E11.75 embryos but did not observe any embryo with an HPE-like phenotype. We did observe some deformed dead embryos. We genotyped all live and dead embryos. The percentages of dead embryos were not significantly different between *Tgif*^{-/-} and *Tgif*^{+/-} embryos (Fig. 5). These results suggest that *Tgif*^{-/-} embryos were not more susceptible to ATRA-induced teratogenic effects.

Expression of the *Tgif* paralogue, *Tgif2*, in *Tgif*^{-/-} mice. Because Tgif has closely related family members, we investigated whether any of these shared expression that might suggest redundant function with Tgif. There are three *Tgif* paralogues in the mouse genome. *Tgif2*, the closest family member of *Tgif*, is on chromosome 2; and *Tgiflx* and *Tgifyt*, two remotely homologous genes, are on the sex chromosomes (6, 21). Since there was no sex differentiation in the phenotype of *Tgif*^{-/-} mice, we focused our attention on *Tgif2*.

Like TGIF, TGIF2 binds Smad and HDAC, playing the role of a corepressor in the TGF- β signaling pathway (31). The homeodomains of TGIF and TGIF2 demonstrate 77% identity, but the similarity is only 49% outside of the homeodo-

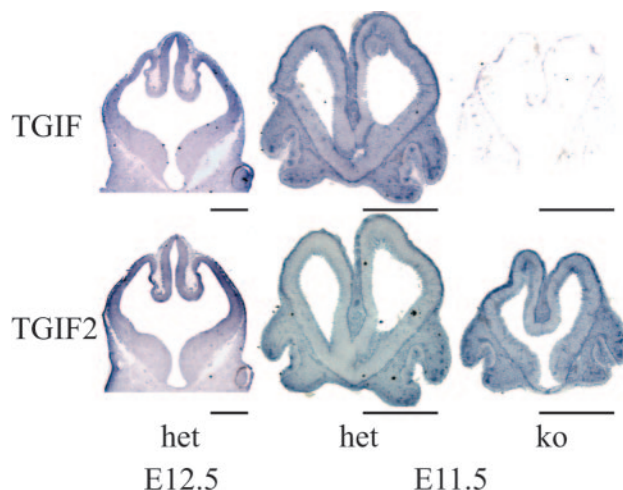


FIG. 6. *Tgif2* expression pattern is similar to that of *Tgif*. At E12.5, *Tgif2* mRNA is expressed in the ventricular neuroepithelium in a similar pattern to *Tgif*. The expression is highest in the cortex and gradually decreases laterally towards the ganglionic eminences. At E11.5, the expression pattern of *Tgif2* is similar to that of *Tgif*. *Tgif2* expression is maintained in *Tgif*^{-/-} embryos, where *Tgif* expression is absent. Scale bars, 1 mm.

main. TGIF2 is slightly smaller, with 237 amino acids, an expected molecular mass of 25.9 kDa, and a pI (isoelectric point) of 7.96, in comparison to the 272-amino-acid TGIF, with a molecular mass of 29.7 kDa and a pI of 8.06, calculated by Lasergene Protean v5.07 (DNASTAR, Madison, WI).

By ISH, we observed that *Tgif2* mRNA was expressed in a similar pattern in the proliferating neuroepithelium to that of *Tgif* at E11.5 and E12.5 (Fig. 6). Interestingly, *Tgif2* expression also displayed a medial to lateral gradient at E12.5. While *Tgif* expression was absent in *Tgif*^{-/-} embryos, *Tgif2* expression was unaltered. Thus, *Tgif2* is coexpressed with *Tgif* and hence could compensate functionally for loss of *Tgif*.

DISCUSSION

Heterozygous *TGIF* mutations in humans have been associated with HPE, and we report here that the spatiotemporal expression profile of *Tgif* is consistent with its potential role in forebrain patterning and proliferation in mice. Surprisingly, however, complete loss of the Tgif protein did not result in HPE in mice.

Several TGIF paralogues are present in the mammalian genome. Human *TGIF2* is located on chromosome 20, and mouse *Tgif2* is located on chromosome 2 (UCSC Genome Browser). *TGIFLX* and *TGIFLY* are two *TGIF*-like genes on the sex chromosomes (6). Our results showed that there was no bias in the sex ratio of *Tgif*^{-/-} mice, suggesting that *Tgiflx* and *Tgifyt* are not the compensating products. On the other hand, *Tgif2* shares high homology with *Tgif* in the TALE homeodomain, which is the DNA binding domain of homeoproteins, suggesting that *Tgif* and *Tgif2* may bind to similar DNA sequences (21). TGIF2 has also been shown to interact with Smad2 and Smad3 as a corepressor (31). Our results showed that the expression pattern of *Tgif2* was strikingly similar to that of *Tgif*, and *Tgif2* expression was maintained in *Tgif*^{-/-}

mice. Therefore, *Tgif2* may compensate for the loss of *Tgif* function.

It remains unclear whether the seven heterozygous mutations in human *TGIF* cause haplo-insufficiency due to partial loss of *TGIF* function, have a dominant-negative effect, or produce novel abnormal functions. Although *TGIF* is partially lost in chromosome 18 deletion cases, the patients also lack other genes in the adjacent genomic region. Therefore, the molecular mechanism may be more complicated in these cases than partial loss of *TGIF* function. Since none of the *TGIF* mutations found to date leads to complete loss of *TGIF*, the mutated *TGIF* may have a dominant-negative effect, which will not only eliminate normal *TGIF* function but also interfere with the function of other *TGIF*-like proteins, such as *TGIF2* (1, 8, 16). Alternatively, a gain-of-function mechanism may underlie the etiology of HPE4. *TGIF* is a Smad corepressor that potentially antagonizes the functions of Nodal, a TGF- β family member, and Smad2. HPE-like phenotypes occur in *Smad2*^{-/-} and *Smad2*^{+/-}; *Nodal*^{+/-} mouse embryos (19, 38). Therefore, *TGIF* mutations in human HPE patients may over-repress the downstream target genes in the Nodal signaling pathway.

It is conceivable that having mutated forms of the *TGIF* protein may be more detrimental than complete loss of the protein. *TGIF* has been shown to autoregulate its own expression level (11). The human *TGIF* promoter region contains TGF- β -responsive elements. *TGIF* represses the transcriptional activation of its own promoter by TGF- β signaling, thus maintaining balanced expression levels of TGF- β target genes. As a result, partial loss of wild-type *TGIF* may lead to over-production of mutated *TGIF*, which interferes with normal developmental processes. In the event of total loss of *TGIF*, there is no mutated *TGIF*. Therefore, normal forebrain patterning may still take place in *Tgif* null mice with a little help from other compensating genes.

HPE is an extremely heterogeneous disease. It has been proposed that it is a multigenic disorder (34). Since currently identified HPE genes only account for a small portion of all sporadic HPE cases, there are still unidentified disease genes. The difficulties in identifying these genes may relate to the multigenic nature of HPE. Loss of function in a single HPE gene may not lead to the disease. In human HPE4 patients, there may be other modifier genes in addition to *TGIF* mutations.

It is well established that environmental and epigenetic factors contribute to the etiology of HPE. The normal-appearing *Tgif*^{-/-} mice may be predisposed to certain environmental conditions that increase the frequency of HPE, although our data with retinoic acid did not reveal such an effect. Therefore, *Tgif*^{-/-} mice can still be a good mouse model to screen for modifier genes with a "second hit" mutation to cause HPE, which is not possible with other early-lethal HPE mouse models.

ACKNOWLEDGMENTS

This work was supported in part by National Institute of Neurological Disorders and Stroke grant R01NS032457 to C.A.W. and by National Cancer Institute grant R24CA83034, a shared resource to Beth Israel Deaconess Medical Center administered by Daniel G. Tenen. C.A.W. is an Investigator of the Howard Hughes Medical Institute. J.S. is a Stuart H. Q. & Victoria Quan Fellow.

We thank members of the Walsh laboratory for their input throughout the course of this project, Clifford Tabin for the mouse *Shh* cDNA plasmid, Susan Dymecki for the FLP deleter mice, Margaret Thompson for the 129 genomic library, Urs Berger for the help with the ISH, Roderick Bronson for consultation on histology, Susanne White for help with histology, and Massachusetts General Hospital Gene Targeting Core for ES cell work and microinjections.

REFERENCES

1. Aguilera, C., C. Dubourg, J. Attia-Sobol, J. Vigneron, M. Blayau, L. Pasquier, L. Lazaro, S. Odent, and V. David. 2003. Molecular screening of the *TGIF* gene in holoprosencephaly: identification of two novel mutations. *Hum. Genet.* **112**:131–134.
2. Ayyar, S., J. Jiang, A. Collu, H. White-Cooper, and R. A. White. 2003. Drosophila *TGIF* is essential for developmentally regulated transcription in spermatogenesis. *Development* **130**:2841–2852.
3. Belloni, E., M. Muenke, E. Roessler, G. Traverso, J. Siegel-Bartelt, A. Frumkin, H. F. Mitchell, H. Donis-Keller, C. Helms, A. V. Hing, H. H. Heng, B. Koop, D. Martindale, J. M. Rommens, L. C. Tsui, and S. W. Scherer. 1996. Identification of Sonic hedgehog as a candidate gene responsible for holoprosencephaly. *Nat. Genet.* **14**:353–356.
4. Bertolino, E., B. Reimund, D. Wildt-Perinic, and R. G. Clerc. 1995. A novel homeobox protein which recognizes a TGT core and functionally interferes with a retinoid-responsive motif. *J. Biol. Chem.* **270**:31178–31188.
5. Bertolino, E., S. Wildt, G. Richards, and R. G. Clerc. 1996. Expression of a novel murine homeobox gene in the developing cerebellar external granular layer during its proliferation. *Dev. Dyn.* **205**:410–420.
6. Blanco-Arias, P., C. A. Sargent, and N. A. Affara. 2002. The human-specific Yp11.2/Xq21.3 homology block encodes a potentially functional testis-specific *TGIF*-like retroposon. *Mamm. Genome.* **13**:463–468.
7. Brown, S. A., D. Warburton, L. Y. Brown, C. Y. Yu, E. R. Roeder, S. Stengel-Rutkowski, R. C. Hennekam, and M. Muenke. 1998. Holoprosencephaly due to mutations in *ZIC2*, a homologue of *Drosophila* odd-paired. *Nat. Genet.* **20**:180–183.
8. Chen, C. P., S. R. Chern, S. H. Du, and W. Wang. 2002. Molecular diagnosis of a novel heterozygous 268C→T (R90C) mutation in *TGIF* gene in a fetus with holoprosencephaly and premaxillary agenesis. *Prenatal Diagn.* **22**:5–7.
9. Chen, C. P., S. R. Chern, C. C. Lee, L. F. Chen, D. T. Chin, C. Y. Tzen, and W. Wang. 2003. Prenatal diagnosis of trisomy 18p and distal 21q22.3 deletion. *Prenatal Diagn.* **23**:758–761.
10. Chen, C. P., S. R. Chern, W. Wang, C. C. Lee, W. L. Chen, L. F. Chen, T. Y. Chang, and C. Y. Tzen. 2001. Prenatal diagnosis of partial monosomy 18p(18p11.2→pter) and trisomy 21q(21q22.3→qter) with alobar holoprosencephaly and premaxillary agenesis. *Prenatal Diagn.* **21**:346–350.
11. Chen, F., K. Ogawa, R. P. Nagarajan, M. Zhang, C. Kuang, and Y. Chen. 2003. Regulation of TG-interacting factor by transforming growth factor- β . *Biochem. J.* **371**:257–263.
12. Chiang, C., Y. Litingtung, E. Lee, K. E. Young, J. L. Corden, H. Westphal, and P. A. Beachy. 1996. Cyclopia and defective axial patterning in mice lacking Sonic hedgehog gene function. *Nature* **383**:407–413.
13. Croen, L. A., G. M. Shaw, and E. J. Lammer. 1996. Holoprosencephaly: epidemiologic and clinical characteristics of a California population. *Am. J. Med. Genet.* **64**:465–472.
14. Echelard, Y., D. J. Epstein, B. St-Jacques, L. Shen, J. Mohler, J. A. McMahon, and A. P. McMahon. 1993. Sonic hedgehog, a member of a family of putative signaling molecules, is implicated in the regulation of CNS polarity. *Cell* **75**:1417–1430.
15. Ferland, R. J., T. J. Cherry, P. O. Preware, E. E. Morrissey, and C. A. Walsh. 2003. Characterization of *Foxp2* and *Foxp1* mRNA and protein in the developing and mature brain. *J. Comp. Neurol.* **460**:266–279.
16. Gripp, K. W., D. Wotton, M. C. Edwards, E. Roessler, L. Ades, P. Meinecke, A. Richieri-Costa, E. H. Zackai, J. Massague, M. Muenke, and S. J. Elledge. 2000. Mutations in *TGIF* cause holoprosencephaly and link NODAL signaling to human neural axis determination. *Nat. Genet.* **25**:205–208.
17. Habedank, M., and G. Trost-Brinkhues. 1983. Monosomy 18p and pure trisomy 18p in a family with translocation (7;18). *J. Med. Genet.* **20**:377–379.
18. Heery, D. M., B. Pierrat, H. Gronemeyer, P. Chambon, and R. Losson. 1994. Homo- and heterodimers of the retinoid X receptor (RXR) activated transcription in yeast. *Nucleic Acids Res.* **22**:726–731.
19. Heyer, J., D. Escalante-Alcalde, M. Lia, E. Boettinger, W. Edelman, C. L. Stewart, and R. Kucherlapati. 1999. Postgastrulation *Smad2*-deficient embryos show defects in embryo turning and anterior morphogenesis. *Proc. Natl. Acad. Sci. USA* **96**:12595–12600.
20. Hyman, C. A., L. Bartholin, S. J. Newfield, and D. Wotton. 2003. Drosophila *TGIF* proteins are transcriptional activators. *Mol. Cell. Biol.* **23**:9262–9274.
21. Imoto, I., A. Pimkhaokham, T. Watanabe, F. Saito-Ohara, E. Soeda, and J. Inazawa. 2000. Amplification and overexpression of *TGIF2*, a novel homeobox gene of the TALE superclass, in ovarian cancer cell lines. *Biochem. Biophys. Res. Commun.* **276**:264–270.
22. Kretschmar, M., and J. Massague. 1998. SMADs: mediators and regulators of TGF- β signaling. *Curr. Opin. Genet. Dev.* **8**:103–111.

23. Kurokawa, R., J. DiRenzo, M. Boehm, J. Sugarman, B. Gloss, M. G. Rosenfeld, R. A. Heyman, and C. K. Glass. 1994. Regulation of retinoid signalling by receptor polarity and allosteric control of ligand binding. *Nature* **371**:528–531.
24. Lagutin, O. V., C. C. Zhu, D. Kobayashi, J. Topczewski, K. Shimamura, L. Puelles, H. R. Russell, P. J. McKinnon, L. Solnica-Krezel, and G. Oliver. 2003. Six3 repression of Wnt signaling in the anterior neuroectoderm is essential for vertebrate forebrain development. *Genes Dev.* **17**:368–379.
25. Lazaro, L., C. Dubourg, L. Pasquier, F. Le Duff, M. Blayau, M. R. Durou, A. T. de la Pintièrre, C. Aguilèlla, V. David, and S. Odent. 2004. Phenotypic and molecular variability of the holoprosencephalic spectrum. *Am. J. Med. Genet.* **129A**:21–24.
26. Leonard, N. J., D. J. Tomkins, and N. Demianczuk. 2000. Prenatal diagnosis of holoprosencephaly (HPE) in a fetus with a recombinant (18)dup(18q)inv(18)(p11.31q11.2)mat. *Prenatal Diagn.* **20**:947–949.
27. Lo, R. S., D. Wotton, and J. Massague. 2001. Epidermal growth factor signaling via Ras controls the Smad transcriptional co-repressor TGIF. *EMBO J.* **20**:128–136.
28. Massague, J. 1998. TGF-beta signal transduction. *Annu. Rev. Biochem.* **67**:753–791.
29. Massague, J., and D. Wotton. 2000. Transcriptional control by the TGF-beta/Smad signaling system. *EMBO J.* **19**:1745–1754.
30. Matsunaga, E., and K. Shioita. 1977. Holoprosencephaly in human embryos: epidemiologic studies of 150 cases. *Teratology* **16**:261–272.
31. Melhuish, T. A., C. M. Gallo, and D. Wotton. 2001. TGIF2 interacts with histone deacetylase 1 and represses transcription. *J. Biol. Chem.* **276**:32109–32114.
32. Melhuish, T. A., and D. Wotton. 2000. The interaction of the carboxyl terminus-binding protein with the Smad corepressor TGIF is disrupted by a holoprosencephaly mutation in TGIF. *J. Biol. Chem.* **275**:39762–39766.
33. Ming, J. E., M. E. Kaupas, E. Roessler, H. G. Brunner, M. Golabi, M. Tekin, R. F. Stratton, E. Sujansky, S. J. Bale, and M. Muenke. 2002. Mutations in PATCHED-1, the receptor for SONIC HEDGEHOG, are associated with holoprosencephaly. *Hum. Genet.* **110**:297–301.
34. Ming, J. E., and M. Muenke. 2002. Multiple hits during early embryonic development: digenic diseases and holoprosencephaly. *Am. J. Hum. Genet.* **71**:1017–1032.
35. Monuki, E. S., F. D. Porter, and C. A. Walsh. 2001. Patterning of the dorsal telencephalon and cerebral cortex by a roof plate-Lhx2 pathway. *Neuron* **32**:591–604.
36. Moog, U., C. E. De Die-Smulders, C. T. Schrandt-Stumpel, J. J. Engelen, A. J. Hamers, S. Frints, and J. P. Fryns. 2001. Holoprosencephaly: the Maastricht experience. *Genet. Couns.* **12**:287–298.
37. Nagai, T., J. Aruga, O. Minowa, T. Sugimoto, Y. Ohno, T. Noda, and K. Mikoshiba. 2000. Zic2 regulates the kinetics of neurulation. *Proc. Natl. Acad. Sci. USA* **97**:1618–1623.
38. Nomura, M., and E. Li. 1998. Smad2 role in mesoderm formation, left-right patterning and craniofacial development. *Nature* **393**:786–790.
39. Olsen, C. L., J. P. Hughes, L. G. Youngblood, and M. Sharpe-Stimac. 1997. Epidemiology of holoprosencephaly and phenotypic characteristics of affected children: New York State, 1984–1989. *Am. J. Med. Genet.* **73**:217–226.
40. Overhauser, J., H. F. Mitchell, E. H. Zackai, D. B. Tick, K. Rojas, and M. Muenke. 1995. Physical mapping of the holoprosencephaly critical region in 18p11.3. *Am. J. Hum. Genet.* **57**:1080–1085.
41. Roach, E., W. Demyer, P. M. Conneally, C. Palmer, and A. D. Merritt. 1975. Holoprosencephaly: birth data, genetic and demographic analyses of 30 families. *Birth Defects Orig. Artic. Ser.* **11**:294–313.
42. Rozen, S., and H. J. Skaletsky. 2000. Primer3 on the WWW for general users and for biologist programmers, p. 365–386. *In* S. Krawetz and S. Misener (ed.), *Bioinformatics methods and protocols: methods in molecular biology*. Humana Press, Totowa, N.J.
43. Seo, S. R., F. Lallemand, N. Ferrand, M. Pessah, S. L'Hoste, J. Camonis, and A. Atfi. 2004. The novel E3 ubiquitin ligase Tiul1 associates with TGIF to target Smad2 for degradation. *EMBO J.* **23**:3780–3792.
44. Sharma, M., and Z. Sun. 2001. 5'TG3' interacting factor interacts with Sin3A and represses AR-mediated transcription. *Mol. Endocrinol.* **15**:1918–1928.
45. Shi, Y., and J. Massague. 2003. Mechanisms of TGF-beta signaling from cell membrane to the nucleus. *Cell* **113**:685–700.
46. Sulik, K. K., D. B. Dehart, J. M. Rogers, and N. Chernoff. 1995. Teratogenicity of low doses of all-trans retinoic acid in presomite mouse embryos. *Teratology* **51**:398–403.
47. Wallis, D. E., E. Roessler, U. Hehr, L. Nanni, T. Wiltshire, A. Richieri-Costa, G. Gillesen-Kaesbach, E. H. Zackai, J. Rommens, and M. Muenke. 1999. Mutations in the homeodomain of the human SIX3 gene cause holoprosencephaly. *Nat. Genet.* **22**:196–198.
48. Wang, Z., and R. S. Mann. 2003. Requirement for two nearly identical TGIF-related homeobox genes in Drosophila spermatogenesis. *Development* **130**:2853–2865.
49. Wotton, D., P. S. Knoepfler, C. D. Laherty, R. N. Eisenman, and J. Massague. 2001. The Smad transcriptional corepressor TGIF recruits mSin3. *Cell Growth Differ.* **12**:457–463.
50. Wotton, D., R. S. Lo, S. Lee, and J. Massague. 1999. A Smad transcriptional corepressor. *Cell* **97**:29–39.
51. Wotton, D., R. S. Lo, L. A. Swaby, and J. Massague. 1999. Multiple modes of repression by the Smad transcriptional corepressor TGIF. *J. Biol. Chem.* **274**:37105–37110.
52. Wurster-Hill, D. H., J. M. Marin-Padilla, J. B. Moeschler, J. P. Park, and M. McDermet. 1991. Trisomy 18 and 18p- features in a case of isochromosome 18q [46,XY,i(18q)]: prenatal diagnosis and autopsy report. *Clin. Genet.* **39**:142–148.
53. Zhang, X., A. Friedman, S. Heaney, P. Purcell, and R. L. Maas. 2002. Meis homeoproteins directly regulate Pax6 during vertebrate lens morphogenesis. *Genes Dev.* **16**:2097–2107.